Science Advances
AAAS

advances.sciencemag.org/cgi/content/full/6/3/eaaz1377/DC1

Supplementary Materials for

The 22 December 2018 tsunami from flank collapse of Anak Krakatau volcano during eruption

Lingling Ye*, Hiroo Kanamori, Luis Rivera, Thorne Lay, Yu Zhou, Dimas Sianipar, Kenji Satake

*Corresponding author. Email: yelingling@mail.sysu.edu.cn

Published 15 January 2020, *Sci. Adv.* **6**, eaaz1377 (2020)
DOI: 10.1126/sciadv.aaz1377

This PDF file includes:

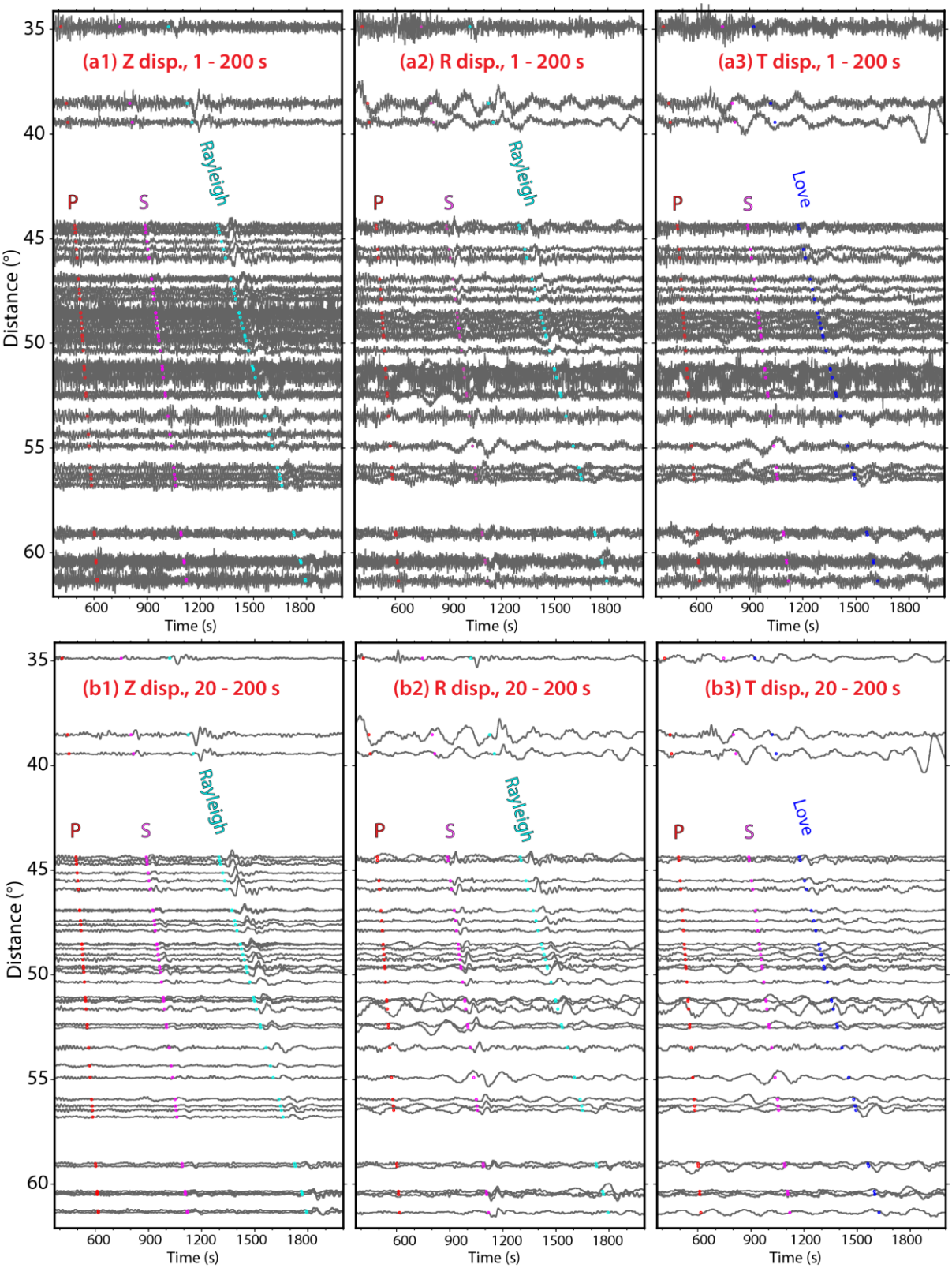

Fig. S1. F-net ground displacements in Japan for time windows of 370 to 2000 s after 13:55:48.7 on 22 December 2018 (UTC). (a1-a3) and (b1-b3) are vertical, radial and tangential ground displacements filtered in the period bands of 1-200 s and 20-200 s, respectively. Red, pink, cyan and blue dots indicate the predicted arrivals of *P*, *S*, Rayleigh (assuming group velocity of 3.8 km/s) and Love (assuming group velocity of 4.2 km/s) waves from a source at Anak Krakatau, respectively.

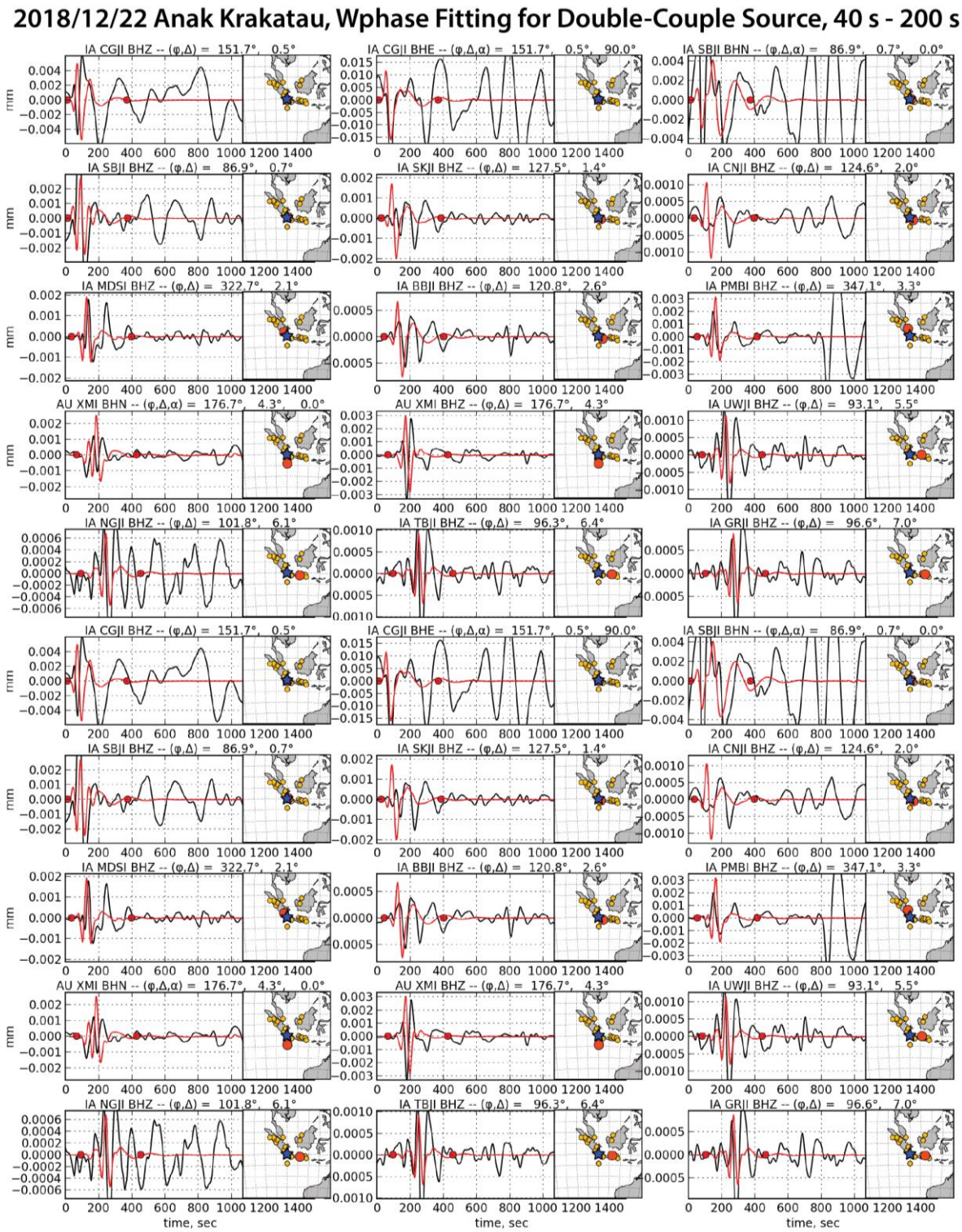

Fig. S2. Regional *W*-phase waveform fits for the moment-tensor source in Fig. 4A. Data (black) and synthetic (red) waveforms are filtered in the period band of 40-200 s. Waveform in the time window bounded by the two red dots are the data used for the inversion. In each insert map, the blue star is the epicenter of the source, the large red circle corresponds to the specific station with waveform shown to its left, and small orange circles indicate all stations used for the inversion.

Fig. S3. Moment-tensor inversion using regional waveforms in the passband 30 to 83 s. The top figure shows the inverted moment-tensor and the lower panel shows waveform fits with data (black) and synthetic (red) filtered in the period band of 30-83.3 s. Other symbols are same as fig. S2.

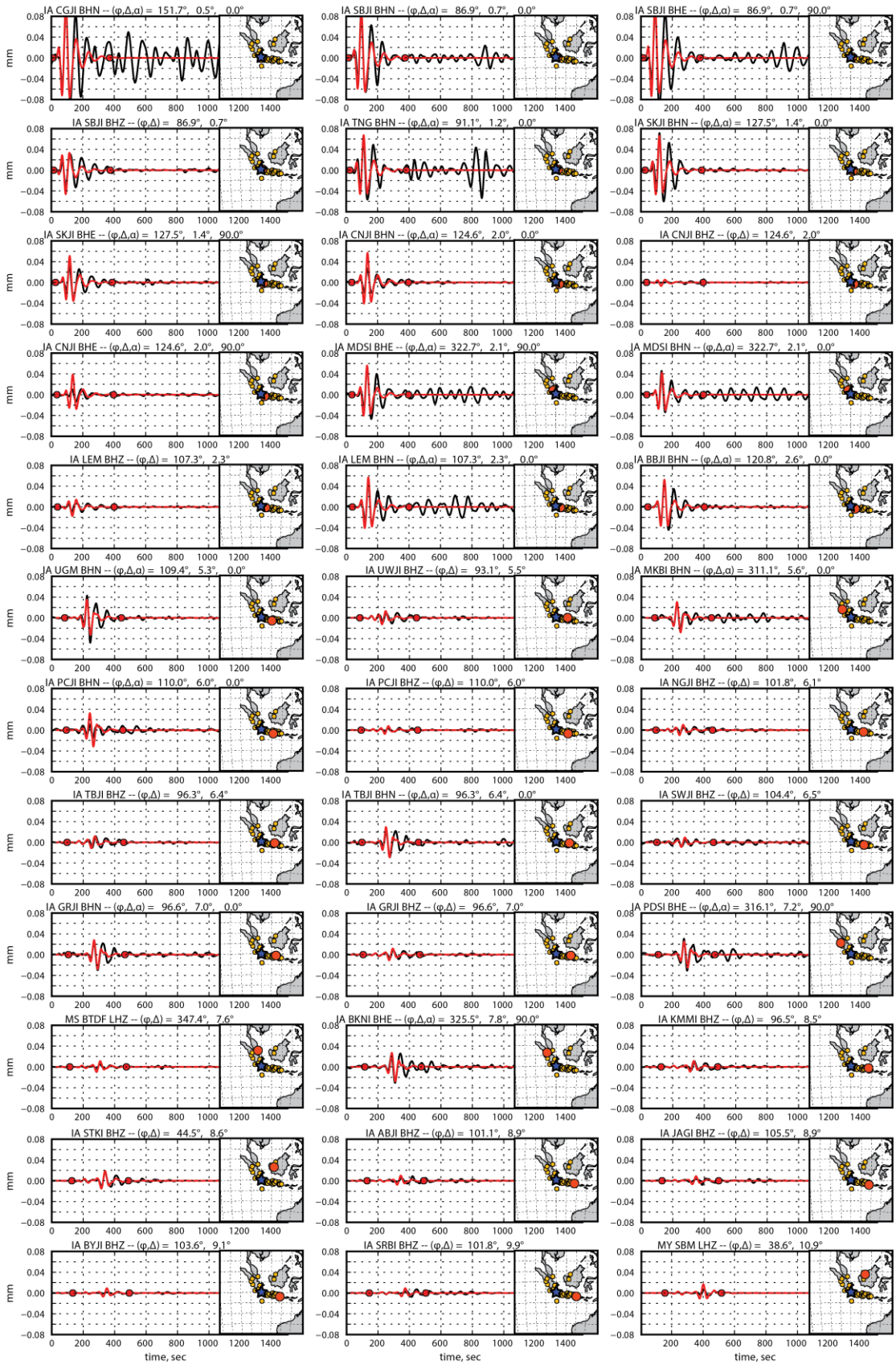

Fig. S4. Waveform fits for the single-force source model in Fig. 4B. Data (black) and synthetic (red) waveforms are filtered in the period band of 30-83.3 s. Other symbols are same as fig. S2.

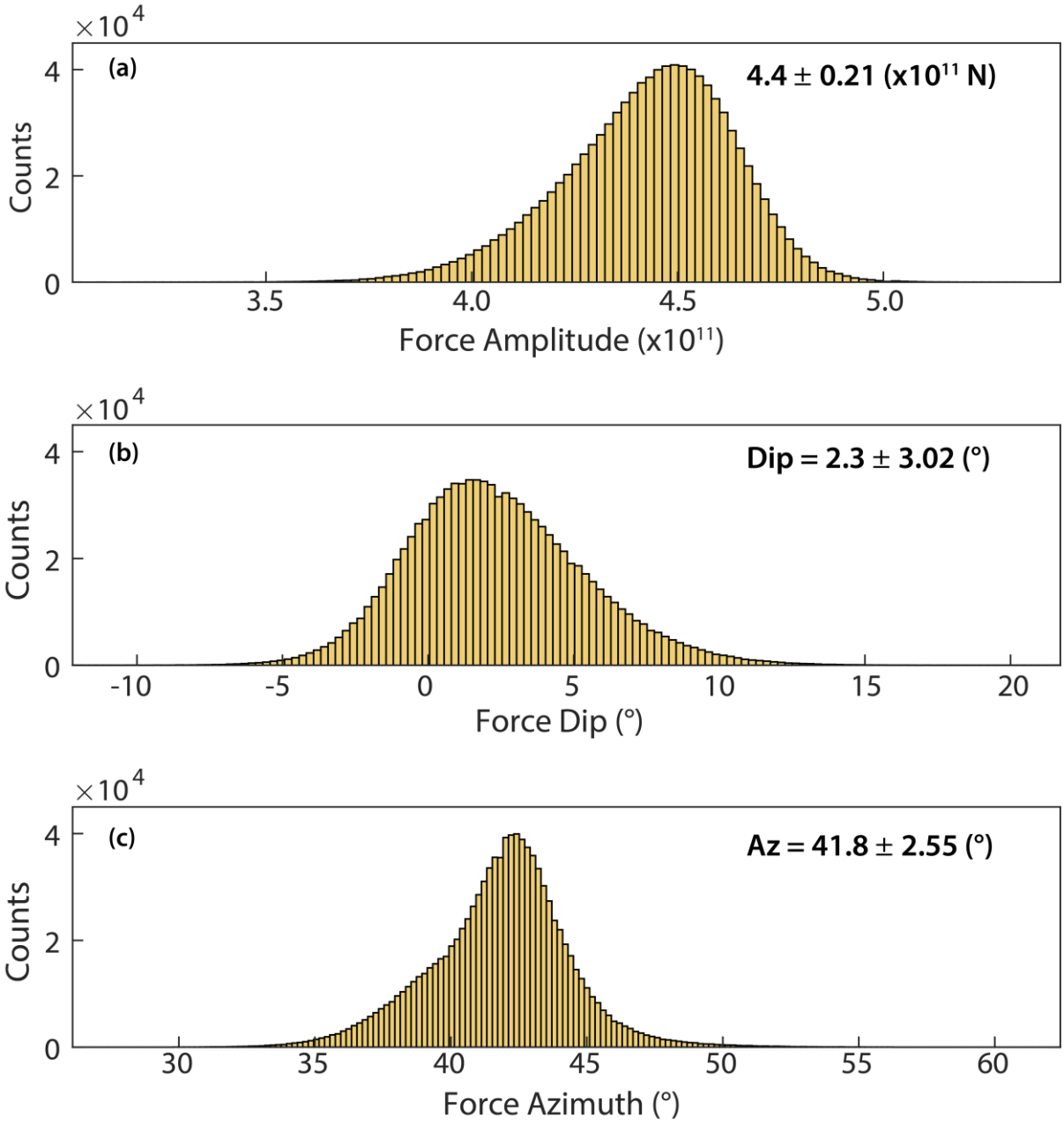

Fig. S5. Bootstrap results for 1,000,000 single-force regional waveform inversions. (a), (b) and (c) are histograms of estimated force amplitude, dip and azimuth of the inverted sources from randomly selecting a random number subset of waveforms from a total dataset of 98 good signal-to-noise traces. A period range of 30-83.3 s is used in every case.

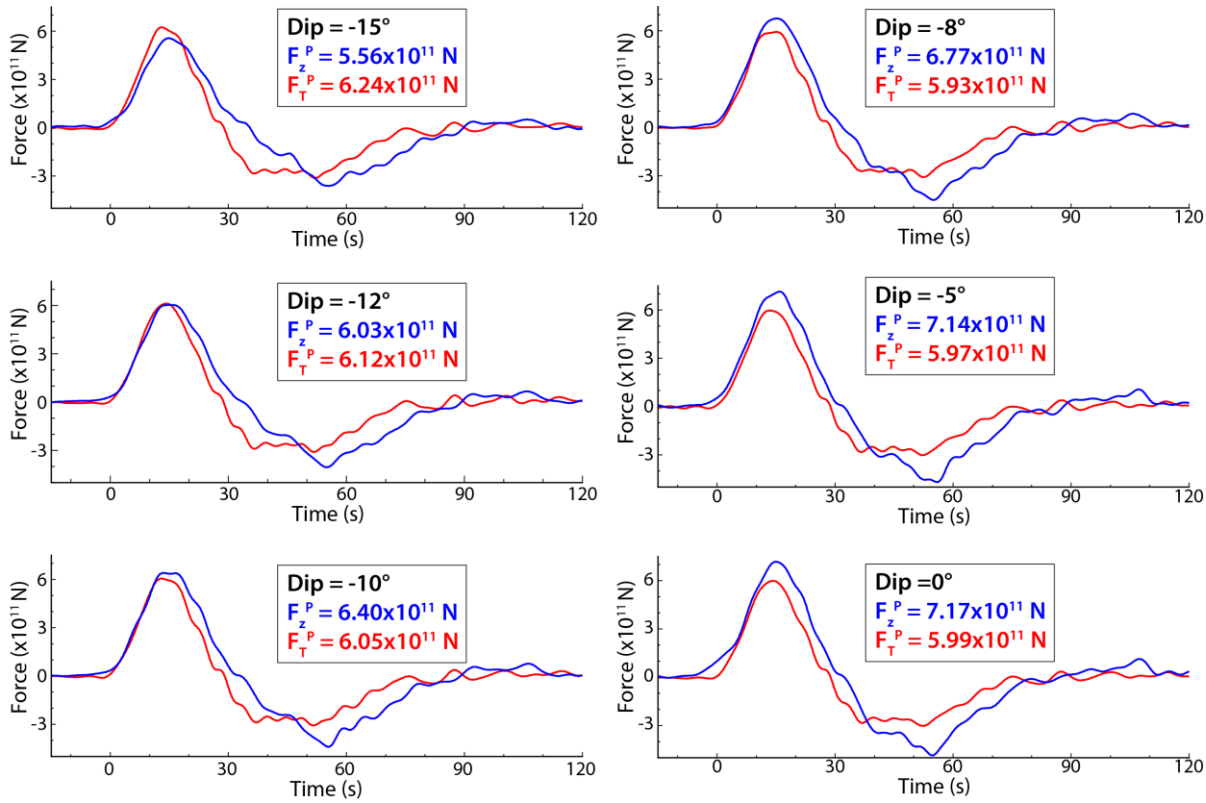

Fig. S6. Stacked force-time history for variable dip angles. Red (tangential) and blue (vertical) curves are linearly stacked force time histories from the deconvolved tangential and vertical components for the indicated dip angle. The same data set as shown in Fig. 5 is used in each case. The force azimuth is held fixed at 42°. The average peak force, F_Z^P and F_T^P for the vertical and tangential components, respectively, inferred from the data stacks are shown in each case, and used to plot Fig. 5b. Note that a dip of -12° gives the best consistency in force inferred from the first peaks of the deconvolved time series.

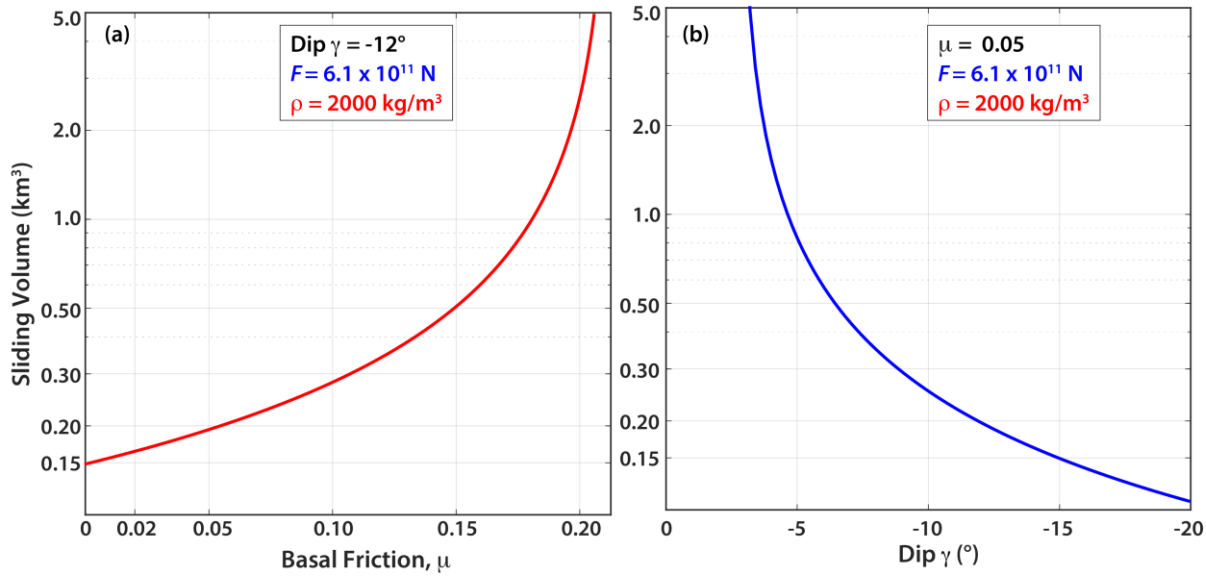

Fig. S7. Estimated slide volume as functions of average basal friction and average detachment dip angle. (a) Estimated slide volume as a function of average basal friction, μ, for a specified single-force amplitude, an effective slide mass density of 2000 km/m^3, and an average single-force dip of -12°. (b) Estimated slide volume for varying single-force dip assuming a fixed basal friction of $\mu = 0.05$, a specified single-force amplitude, and an effective slide mass density of 2000 kg/m^3.

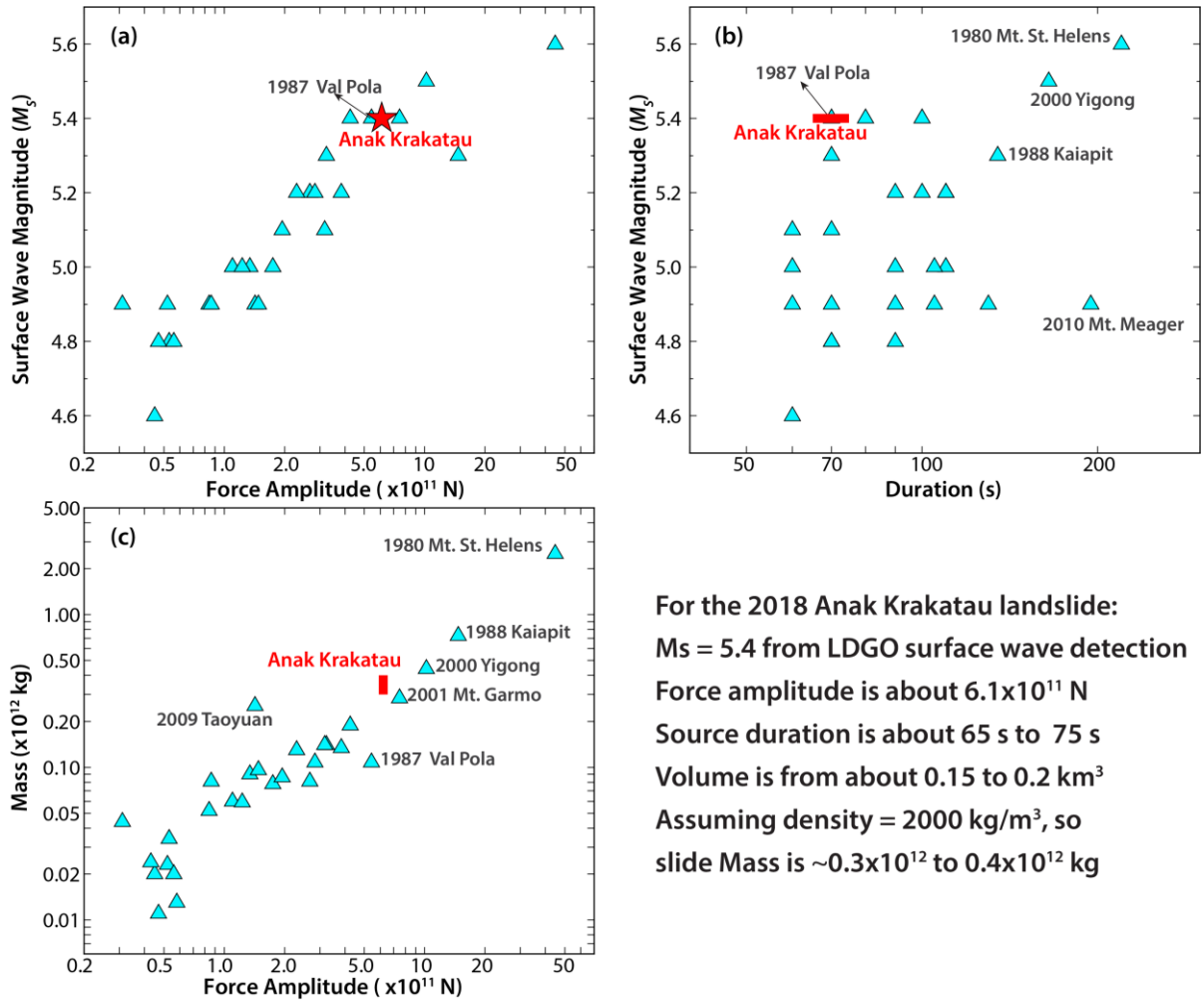

Fig. S8. Comparison of key estimates of the 2018 Anak Krakatau landslide with other landslides. (a) Single-force amplitude versus surface wave magnitude; (b) Source duration versus surface wave magnitude; (c) Force amplitude versus slide mass. Cyan triangles are measurements from Ekström and Stark (2013).